Molecular Structure of Metallocene-Catalyzed Polyethylene: Rheologically Relevant Representation of Branching Architecture in Single Catalyst and Blended Systems

Stephane Costeux, Paula Wood-Adams,* and Daryoosh Beigzadeh†

Department of Chemical Engineering, McGill University, Montreal, Quebec

Received August 9, 2001; Revised Manuscript Received January 7, 2002

ABSTRACT: The goal of this work was to provide a usable framework for describing the molecular structure of long-chain branched, metallocene-catalyzed polyethylene (mPE). This will allow better understanding of structure−property relations for these materials and in the future allow the development of new metallocene based systems with tailor-made properties. In particular, we are interested in the relationship between molecular structure and rheological behavior of polyethylene and therefore represent the structure in terms that are relevant to the rheological properties. To provide an intuitive understanding of the structure, we present a ternary diagram showing clearly the independent variables in the system and allowing a quick analysis of blended systems.

Introduction

One of the greatest challenges in the development of structure−property relations for polymeric materials lies in the meaningful characterization of molecular structure. Various analytical measures are available for different aspects of polymer molecular structure, and it is necessary to bring this information together in an appropriate way. The analytical measures of course all have certain limitations, and none of them provide the whole story in a single parameter or even in a single distribution.

This is particularly true in the case of long chain branched polymers. To fully characterize the molecular structure of long chain branched polymers one must have information about the molecular weight distribution of the whole polymer, the branch point density, and the branching structure. One can obtain a reasonable estimate of the molecular weight distribution using appropriate size exclusion chromatography techniques and of the branch point density using ^{13}C nuclear magnetic resonance. It is in the third item that the most difficulty arises, as we do not have a direct measure of branching structure. Instead, we must make use of information about the polymerization reaction mechanism to determine the branching structure, and we must also represent that structure in a useful way.

In this work, we present a protocol for representing the branching architecture of metallocene-catalyzed long chain branched polyethylene. We make use of Monte Carlo simulations to generate sets of molecules with the same statistical properties as the real materials. We then analyze the simulated chains and develop analytical relationships for all of branching statistics in terms of two experimentally measurable average molecular parameters, weight-average molecular weight and average branch point density. We present the general bivariate distributions for these systems as well as all of the necessary equations for the specific aspects of the molecular structure. We propose a new way of illustrating the topology of metallocene polyethylene, and finally, we present guidelines for applying this analysis to blended systems.

Review of Recent Studies of Branching Structure in Metallocene Polyethylene

Soares and Hamielec[1] were the first to describe the kinetics of polymerization of long chain branched mPE by taking into account the four following steps:

$$(1)\ P_{x,n} + M \xrightarrow{k_p} P_{x+1,n}$$

monomer addition

$$(2)\ P_{x,n} + D^{=}_{y,m} \xrightarrow{k_{LCB}} P_{x+y,n+m+1}$$

addition of unsaturated branch

$$(3)\ P_{x,n} + CTA \xrightarrow{k_{CTA}} D^{+}_{x,n} + P_{1,0}$$

generation of dead saturated chains

$$(4)\ P_{x,n} \xrightarrow{k_\beta} D^{=}_{x,n} + P_{1,0}$$

β-hydride elimination

where M denotes a monomer, P a living polymer with catalyst attached at one end, D^+ a saturated dead chain, $D^=$ a vinyl-terminated dead chain that can be grafted as a branch, and CTA a chain transfer agent. Their analysis of the reaction kinetics shows that dead chains, branches, and living polymers all have identical MWDs and that the fractions of each type of chain depends on the rate constants. They also found that all segments respond to Flory statistics, with a polydispersity index of 2. It also provides the distribution of molecular weights and branch points. This analytical solution agrees very well with a Monte Carlo simulation using two probabilities, one for propagation and one for branching. They also predict the LCB per 10^3 C and the branching frequency, $\bar{B}_N$, which is the average number of branches per molecule.

Beigzadeh et al.[2] extended the use of Monte Carlo simulations and showed the importance of comblike and

* Corresponding author. Current address: Department of Mechanical and Industrial Engineering, Concordia University, Room H 549, 1455 de Maisonneuve Blvd. West, Montreal, Quebec, Canada H3G 1M8.

† Current address: The Dow Chemical Co., 1776 Building, Midland, MI 48674.

10.1021/ma011432c CCC: $22.00
Published on Web 02/28/2002

dendritic molecules at the high molecular weight end of the distribution. They suggested that these structures could strongly influence the rheological properties of these materials.

Another analysis of single-site-catalyzed polymerization was presented by Yiannoulakis et al.[3] Their kinetic equations are slightly different from the ones of Soares and Hamielec[1] and are solved for each subset of molecules with different number of branch points per chain. The statistics of the whole system is then obtained by summing the weighted population using a Schultz−Flory distribution, which leads to results identical to those of ref 1.

Read and McLeish[4] revisited the approach of Soares and Hamielec[1] and introduced a new formalism for computing the molecular statistics from the same kinetic equations. Their conclusions and results concerning the distributions of molecular weight and branch points are identical to those of Soares and Hamielec.[1] Read and McLeish[4] also show that in addition to the number-average molecular weight of the strands, which is the same for linear chains and all segments of branched molecules, one single branching parameter is necessary to characterize all the properties of the branched system. This parameter, b^{U}, the upstream branching probability, is related closely to the $\bar{B}_N$ of Soares and Hamielec. Read and McLeish also use seniority to classify segments between branch points, according to their distance from a free end, and priority, which is related to the number of paths leading to a free end. They then make use of the resulting seniority and priority distributions to predict the rheology of these branched mPE systems.

Monte Carlo Based Evaluation of Branch Structure

Beigzadeh et al.[2] proposed a technique for predicting detailed branching structure of metallocene polyethylene using Monte Carlo simulations. In these simulations, molecules are built up monomer by monomer until there are enough molecules present such that the distributions of structures in the system are representative. The molecules are built according to three assumptions:

1. The molecular weight distribution of a purely linear polymer can be represented by the most probable (or Flory) distribution (eq 1).

$$w(M) = \frac{M}{{M_0}^2}(1-p)^2 p^{M/M_0-1} \qquad (1)$$

where p is the extent of reaction. For $p \cong 1$, this distribution has a polydispersity index, M_W/M_N of 2, and has previously been shown to provide a good representation of the molecular weight distribution of linear metallocene polyethylene.

2. The long chain branches are formed by the incorporation of macromonomers as described by Soares and Hamielec.[1]

According to the currently accepted reaction mechanism, any of the molecules in the reaction medium can become macromonomers. In our simulations, we consider all of the previously generated molecules to be potential macromonomers. This approach becomes more representative of reality as the number of simulated molecules increases.

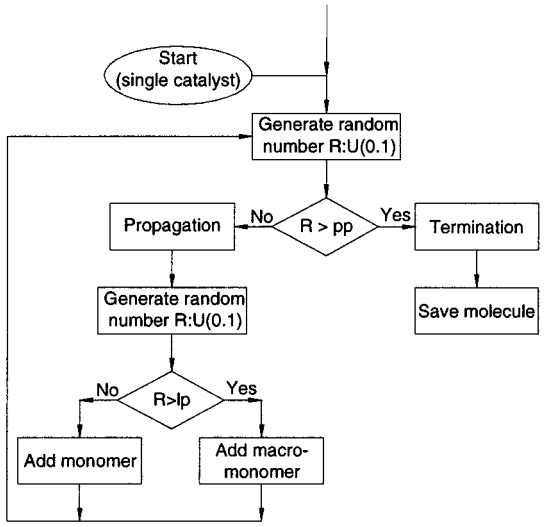

Figure 1. Algorithm for Monte Carlo simulations.

3. The incorporation of a branch in a particular position does not affect the probability of a branch being incorporated in adjacent positions.

In reality, the presence of a long chain branch does reduce the likelihood of another long chain branch being placed in the next position due to steric hindrances. However, at the low level of branching in the materials we are studying, this reduction in probability does not have a significant effect on the Monte Carlo simulations.

Figure 1 shows the Monte Carlo algorithm that we used for single-catalyst systems, which is based on two probabilities: (1) pp, the propagation probability and (2) lp, the monomer selection probability. We derive the exact relations between molecular weight averages and branch point density and the two probabilities in a later section. From the four kinetic equations above, we can define the following reaction rates using the results of Soares and Hamielec:[1] rate of monomer addition, R_M; rate of macromonomer addition, R_{LCB}; and the rate of termination, R_T, which is equal to $R_{CTA} + R_\beta$. We can relate these reaction rates to the Monte Carlo probabilities by recalling that the termination probability is (1 − pp) and the absolute probabilities of adding a monomer or a branch are (pp × lp) and pp × (1 − lp) respectively, which can be related to the rates above after setting $R = R_M + R_{LCB} + R_T$. Then $R_T = R \times (1 - pp)$, $R_M = R \times pp \times lp$ and $R_{LCB} = R \times pp \times (1 - lp)$. Thus, we derive simply $pp = (R_M + R_{LCB})/R$ and $lp = R_M/(R_M + R_{LCB})$.

We performed Monte Carlo simulations over broad ranges of propagation and monomer selection probabilities in order to fully explore the range of structures that can be produced with these catalysts. For each probability combination, approximately 400 000 chains were generated. When building a chain, the lengths of segments of the main backbone were recorded to permit determination of MWD of segments. At the termination of each chain, its total length and number of branch points were recorded, so that if the chain is grafted as a macromonomer, the weight and number of branch points of the new molecule can be computed. The results of the simulations were used to guide and confirm our analytical derivations for the branching statistics and molecular weight distributions. Detailed information on molecules with less than five branch points was also recorded to check the bivariate distributions.

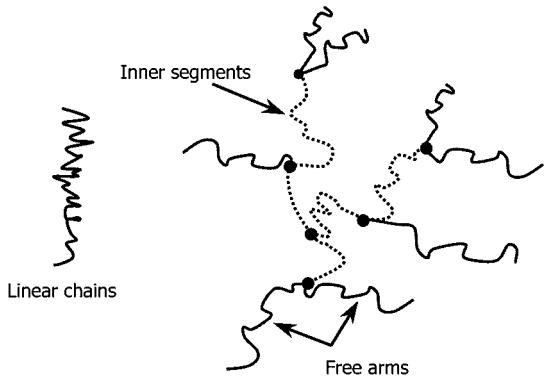

Figure 2. Different types of segments in LCB mPE.

Rheologically Relevant Representation of Branching Structure

The Monte Carlo simulations showed that long chain branched metallocene polyethylenes are mixtures of linear chains and various branched molecules. The linear molecules have a polydispersity index of approximately 2 and the polydispersity index of the molecules with n branch points is given by eq 2.

$$\frac{M_W(n)}{M_N(n)} = \frac{2(n+1)}{2n+1} \tag{2}$$

While these results are interesting, they are not particularly useful for understanding the rheological properties of branched mPE. As pointed out by Read and McLeish,[4] in terms of rheological properties, the different types of segments present in branched mPE are much more important than the different types of molecules (Figure 2). For example, free arms (segments with one free end and one branch point at the other) all relax in the same way, regardless of the total number of branch points on the rest of the molecule. We therefore focus on the various segments in long chain branched mPE.

The first task was to identify the important different kinds of segments in long chain branched metallocene polyethylene. For our analysis we chose to consider three types of segments: linear chains, free arms (one free end and one end at a branch point), and inner segments (both ends at branch points). These types of segments each exhibit different relaxation processes: the linear chains reptate, the free arms retract, and finally the inner segments relax by hindered reptation. This approach is a simplification as not all of the inner segments behave in the same way. In reality, it is the seniority of an inner segment that determines how and when it relaxes stress (in the linear regime). Because of the greatly simplified analysis, we consider long chain branched mPE to be a ternary system of linear chains, free arms, and inner segments.

Our simulations showed that the distributions of molecular weights of these different segments follow the same Flory distribution (Figure 3). This means that the relevant average molecular weight for long chain branched mPE is the number-average segment molecular weight, $M_{N,S}$.

A particularly useful way of representing the topology of long chain branched mPE is in a ternary diagram as in Figure 4. The points were generated by performing

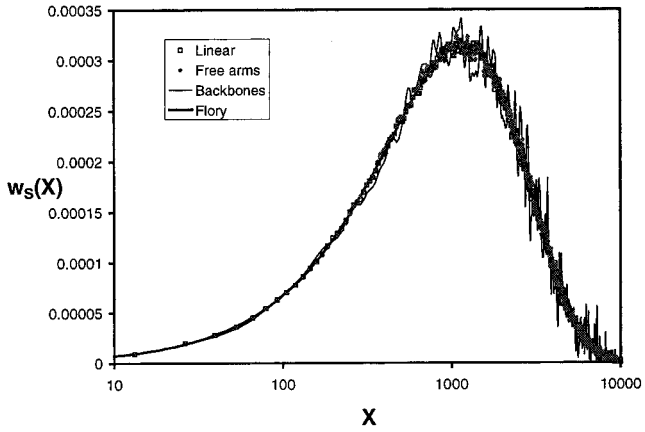

Figure 3. Distribution of molecular weights for linear molecules, free arms, and inner segments (10^6 molecules, pp = 0.999244, lp = 0.9999).

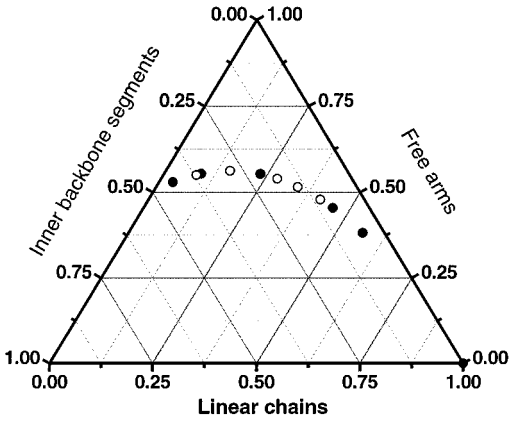

Figure 4. Ternary diagram representation of topology of LCB mPE. Ten simulated samples are represented: five for different lp keeping pp constant (filled dots) and five for different pp and constant lp (open dots).

10 different simulations; the first five with constant propagation probability and varying monomer selection probability and the second five with constant monomer selection probability and varying propagation probability (Table 1). The axes of the ternary diagram are in terms of fraction of segments; for example the lower axis gives the fraction of the segments that are linear chains. Since all types of segments have the same MWD, the composition of the overall system in terms of mass fractions of segments is equal to the composition in terms of number fractions of segments.

The final necessary component to this representation is the parameter that determines the position of a material on the ternary diagram. A convenient choice for this parameter is the average number of branches per molecule, β

$$\beta \equiv \frac{M_N \lambda}{14 \times 10^3} \tag{3}$$

In this equation, M_N is the number-average molecular weight of the whole polymer and λ is the average branch point density per 10^3 C (as measured by ^{13}C NMR). β varies from 0 for linear systems to ∞, which is similar to a percolation threshold (see Appendix D for more discussion on this issue). We note that this definition of β corresponds to a branching density, λ, equal to the total number of branch points divided by the number-

Table 1. Results from Monte Carlo Simulations[a]

no.	pp	lp	β	ϕ_L	ϕ_A	ϕ_B
1	**0.999176**	0.999840	0.243	0.566	0.381	0.052
2	**0.999176**	0.999780	0.367	0.457	0.454	0.089
3	**0.999176**	0.999600	0.953	0.232	0.554	0.214
4	**0.999176**	0.999400	2.688	0.091	0.554	0.356
5	**0.999176**	0.999200	11.918	0.034	0.530	0.436
6	0.999000	**0.999700**	0.433	0.414	0.479	0.107
7	0.999176	**0.999700**	0.577	0.342	0.515	0.143
8	0.999300	**0.999700**	0.756	0.280	0.539	0.181
9	0.999500	**0.999700**	1.469	0.155	0.563	0.282
10	0.999600	**0.999700**	2.719	0.081	0.550	0.369

[a] Note: For high values of β, the simulation does not represent well the real system because only the molecules with less than 1000 branch points are counted. The values for β and ϕ_i presented in this table are obtained by analyzing the simulated chains using eq 3 for β. These results are in accord with the analytical solution with the exception of no. 5 where there are up to 6000 branch points on some molecules and the total number of molecules in the simulation was not sufficient for accurate statistics.

average molecular weight rather than M_W as is sometimes done in experimental studies. This choice will be justified in the next sections.

Analytical Relationships for Average Molecular Weights

In the case of linear metallocene polyethylene, the probability of adding a monomer at any time is equal to the probability of propagation, pp since the monomer selection probability is 1. The probability of obtaining a chain with x monomers, $n(x)$, is equal to the probability of adding $x - 1$ monomers to a monomer before terminating. This leads to the classical Flory distribution

$$n(x) = \mathrm{pp}^{x-1}(1 - \mathrm{pp}) \tag{4}$$

with the following average molecular weights

$$M_N = 28\sum_{x=1}^{\infty} xn(x) = \frac{28}{1 - \mathrm{pp}} \tag{5}$$

$$M_W = 28\frac{\sum_{x=1}^{\infty} x^2 n(x)}{\sum_{x=1}^{\infty} xn(x)} = 28\left(\frac{1 + \mathrm{pp}}{1 - \mathrm{pp}}\right) \tag{6}$$

and a polydispersity index equal to

$$\mathrm{PDI} = \frac{M_W}{M_N} = 1 + \mathrm{pp} \approx 2 \tag{7}$$

A similar analysis can be applied to branched metallocene polyethylene. In this case, the probability of adding a monomer is the product of pp and lp and the probability of adding a macromonomer is pp(1 − lp). Then the number probability of obtaining a segment of x monomers is given by eq 8, the weight probability by eq 9 and the number and weight-average segment molecular weights are given by parts a and b of eq 10.

$$n_S(x) = (\mathrm{pp} \times \mathrm{lp})^{x-1}(1 - \mathrm{pp} \times \mathrm{lp}) \tag{8}$$

$$w_S(x) = x(\mathrm{pp} \times \mathrm{lp})^{x-1}(1 - \mathrm{pp} \times \mathrm{lp})^2 \tag{9}$$

$$M_{N,S} = 28\sum_{x=1}^{\infty} xn_S(x) = \frac{28}{1 - \mathrm{pp} \times \mathrm{lp}} \tag{10a}$$

$$M_{W,S} = 28\frac{\sum_{x=1}^{\infty} x^2 n_S(x)}{\sum_{x=1}^{\infty} xn_S(x)} = 28\left(\frac{1 + \mathrm{pp} \times \mathrm{lp}}{1 - \mathrm{pp} \times \mathrm{lp}}\right) \tag{10b}$$

This means that the segments between branch points obey a Flory type distribution, as shown in Figure 3.

Modification of Monte Carlo Algorithm

This observation that all of the segments follow the same MWD suggests a method for significantly accelerating the simulation. Instead of adding monomer by monomer, one can add segments following the distribution described by eq 8. Random segments following this distribution can be generated by using the cumulative form of eq 8:

$$\mathrm{CN}_S(x) = \sum_{y=1}^{x} n_S(y) = 1 - (\mathrm{pp} \times \mathrm{lp})^x \tag{11}$$

First we choose a random number, r, between 0 and 1, and then the length of the segment, x, corresponding to r is such that

$$\mathrm{CN}_S(x - 1) < r \leq \mathrm{CN}_S(x) \tag{12}$$

as the probability that r falls in this interval is $\mathrm{CN}_S(x) - \mathrm{CN}_S(x - 1) = n_S(x)$. Therefore, the value of x is given by

$$\mathrm{x} = \mathrm{int}\left(\frac{\log(1 - r)}{\log(\mathrm{pp} \times \mathrm{lp})}\right) + 1 \tag{13}$$

The next step is to define the Flory[5] branching probability P_b which is given by the ratio of the probability that a segment will end at a branch point,

pp(1 − lp) and the total probability that a segment will end, (1 − pp × lp).

$$P_b = \frac{pp(1 - lp)}{1 - pp \times lp} \tag{14}$$

We note that this probability is identical to the b^U of Read and McLeish.[4]

Then we pick a second random number R between 0 and 1, and if $R < P_b$, we incorporate a macromonomer or otherwise the chain terminates. The resulting set of molecules is statistically identical to the classical Monte Carlo, leading to identical branch point and weight distributions. This modified algorithm gives much faster computations and makes possible the simulation of 10 million molecules in 2 min on a Pentium III-300 MHz, instead of 30 min to 1 h for the classical Monte Carlo. Moreover, the computation time is independent of the average segment length, which is not true for the original method.

Branching Statistics

The next step is to derive analytical relations for the branching statistics in terms of the two average molecular parameters for which we believe that we have the most accurate measurements: M_W (light scattering) and λ (from NMR). At this point it is useful to take another look at our parameter β, which we are using to describe the branching level of metallocene polyethylene. We now demonstrate that eq 3 is the appropriate definition for the average number of braches per molecule.

We start by writing β as the first moment of the distribution of branch points throughout the molecules:

$$\beta = \sum_{n=0}^{\infty} nF_N(n) \tag{15}$$

$F_N(n)$, the number fraction of chains with n branch points, can be related to the branching probability P_b by considering the number of different ways a molecule with n branch points can be constructed in this system. The function that describes the number of different possibilities for each n is the Catalan number, $C(n)$

$$C(n) = \frac{(2n)!}{n!(n+1)!} \tag{16}$$

which was already obtained by Flory[6] in the case of random gelation of linear chains. The reason for this similarity is explained in Appendix A.

Next we express $F_N(n)$ in terms of the Flory[5] branching probability (the probability that a particular segment ends in a branch point), P_b.

$$F_N(n) = C(n){P_b}^n(1 - P_b)^{n+1} \tag{17}$$

This result can be understood[4] by recalling that when building a molecule with n branch points, starting at a free end, there will be n segments that end at a branch point with probability P_b and $(n + 1)$ free arms that end by termination, each with a probability $1 - P_b$.

Now we can derive the equation for β in terms of the Monte Carlo probabilities. Details are provided in Appendix A.

$$\beta = \sum_{n=0}^{\infty} nF_N(n) = \sum_{n=1}^{\infty} nC(n){P_b}^n(1 - P_b)^{n+1} = \frac{P_b}{1 - 2P_b}$$

$$\beta = \frac{pp(1 - lp)}{1 - 2pp + pp \times lp} \tag{18}$$

To continue, we define another parameter, β_S, which is the average number of segments per molecule.

$$\beta_s = \sum_{n=0}^{\infty} (2n + 1)F_N(n) \tag{19}$$

By combining eqs 15 and 19 we derive eq 20.

$$\beta_S = 2\beta + 1 \tag{20}$$

We can then write the average branch point density, λ, in terms of β and β_S.

$$\lambda = \frac{\text{no. of branch points per molecule}}{\text{no. of segments per molecule}} \times \frac{10^3}{\text{no. of C per segment}} = \left(\frac{\beta}{\beta_S}\right)\frac{14 \times 10^3}{M_{N,S}} \tag{21}$$

Equation 21 can of course be rewritten in terms of the Monte Carlo probabilities.

$$\lambda = \frac{10^3}{2} pp(1 - lp) \tag{22}$$

Now we need to relate the segment molecular weight distribution and the branching statistics to the overall molecular weight distribution of a branched system. The average molecular weights of molecules with n branch points are given by eqs 23 and 24, which are derived in Appendix B.

$$M_N(n) = (2n + 1)M_{N,S} \tag{23}$$

$$M_W(n) = 2(n + 1)M_{N,S} \tag{24}$$

The number-average molecular weight of the whole system is then:

$$M_N = \frac{\sum_{n=0}^{\infty} M_N(n)F_N(n)}{\sum_{n=0}^{\infty} F_N(n)} = (2\beta + 1)M_{N,S} \tag{25}$$

The weight-average molecular weight of the whole system is

$$M_W = \frac{\sum_{n=0}^{\infty} M_N(n)M_W(n)F_N(n)}{\sum_{n=0}^{\infty} M_N(n)F_N(n)} = 2(\beta + 1)(2\beta + 1)M_{N,S} \tag{26}$$

The polydispersity index is thus:

$$\frac{M_W}{M_N} = 2(\beta + 1) \tag{27}$$

We note that although β is apparently identical to the branching parameter B_N of Soares and Hamielec,[1] we find that eq 27 is valid for any value of β whereas the same relation was not valid above $B_N = 0.3$ in ref 1.

Finally, by combining eq 21 and 25, one finds indeed eq 3, the relationship between β and the two average molecular parameters, λ and M_N. A more useful relationship is given in eq 28, which relates β to the two molecular quantities that can be accurately measured.

$$\lambda = \frac{14 \times 10^3 (2\beta)(\beta + 1)}{M_W} \tag{28}$$

Segment Type Statistics

We have presented the results of our Monte Carlo simulations in terms of a ternary system of linear chains, free arms and inner backbone segments. We now present the analytical derivation for the segment statistics. The fraction of segments that are linear chains is equal to the ratio of the number fraction of chains that are linear, $F_N(0)$, to the average number of segments per molecule, β_S.

$$\phi_L = \frac{F_N(0)}{\beta_s} = \frac{(1 - P_b)}{\beta_s} = \frac{\beta + 1}{\beta_s(2\beta + 1)} = \frac{\beta + 1}{(2\beta + 1)^2} \tag{29}$$

A molecule with n branch points will have $(n + 2)$ free arms; therefore, the average number of free arms per molecule is

$$\beta'_A = \sum_{n=0}^{\infty} (n + 2) F_N(n) = \beta + 2 \tag{30}$$

Equation 30 includes linear molecules, $(n = 0)$, which are counted as two free arms. These arms are subtracted to give the average number of free arms per branched molecule:

$$\beta_A = \beta'_A - 2F_N(0) = \beta + 2 - 2\left(\frac{\beta + 1}{2\beta + 1}\right) = \frac{\beta(2\beta + 3)}{2\beta + 1} \tag{31}$$

The fraction of segments that are free arms is equal to the ratio of the average number of free arms per branched molecule to the average number of segments per molecule:

$$\phi_A = \frac{\beta_A}{\beta_S} = \frac{\beta(2\beta + 3)}{(2\beta + 1)^2} \tag{32}$$

Following a similar reasoning we can express the average number of inner backbone segments per branched molecule as in eq 33.

$$\beta_B = \sum_{n=1}^{\infty} (n - 1) F_N(n) = \frac{2\beta^2}{2\beta + 1} \tag{33}$$

Finally, the fraction of the segments that are inner backbone segments is equal to the ratio of the average number of inner backbone segments per branched molecule to the average number of segments per molecule:

$$\phi_B = \frac{2\beta^2}{(2\beta + 1)^2} \tag{34}$$

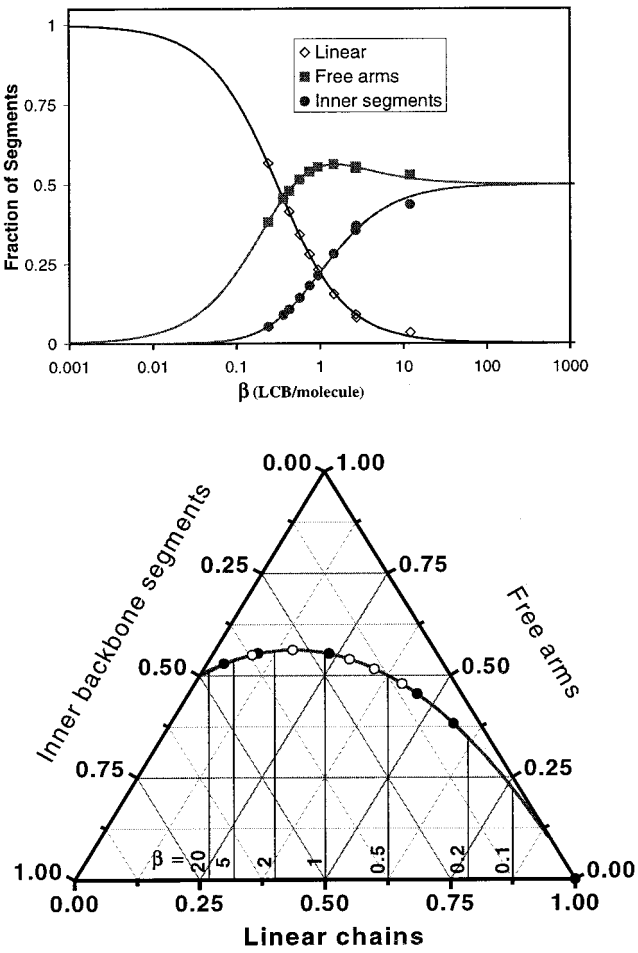

Figure 5. Comparison of analytical solution with simulations: (a) segment type fractions as a function of β on a Cartesian plot and (b) the ternary diagram.

The validity of eqs 30, 32, and 34 is demonstrated by comparing them to the results of the Monte Carlo simulations in Figure 5, parts a and b. The results of the Monte Carlo simulations are also presented in Table 1. As all the segments follow the same Flory distribution (eqs 8−10), the fractions ϕ_L, ϕ_A, and ϕ_B represent segment fractions both in number and weight. In Figure 5b, the continuous line represents the locus of all possible topological composition of single-site metallocene systems.

Domain of Validity of the Topological Model

The model presented above is valid for any value of β. Nevertheless some restrictions exist on the choice of the monomer selection probability, lp, to be able to simulate a real branched metallocene polyethylene. If lp is too small, too many branch points will be created which will consume all molecules by incorporating them as branches, thus leading to a percolation of the system, which actually does not occur for a real system (cf. Appendix D). The restriction on lp is given by the fact that the denominator of β in eq 18 must not become zero,

Table 2. Long Chain Branched MPEs

resin	M_W DRI[a]	M_W LALLS	PDI DRI	PDI LALLS/DRI	LCB/10^3 C ^{13}C NMR	β	$M_{N,S}$	PDI eq 27
HDB1	78 000	77 000	1.98	1.95	0.026	0.067	31 800	2.13
HDB2	80 000	82 000	1.93	1.98	0.037	0.099	31 200	2.20
HDB3	82 000	86 000	1.99	2.09	0.042	0.116	31 300	2.23
HDB4	84 000	96 000	2.14	2.45	0.080	0.224	27 100	2.45

[a] DRI = differential refractive index detector.

which leads to the following condition:

$$\mathrm{lp} > 2 - \frac{1}{\mathrm{pp}} \tag{35}$$

Moreover, we have considered until now that all created chains can be incorporated as macromonomers. This approximation lies in the fact that we simply added the kinetic rates R_{CTA} and R_β to form the rate of termination from which pp was computed. This approach is correct, but in order to completely describe the system, we need to introduce a third parameter, ν, corresponding to the probability of terminating a chain by a vinyl group.

$$\nu = \frac{\mathrm{R}_\beta}{\mathrm{R}_\beta + R_{CTA}} \tag{36}$$

This means that only a fraction, ν, of the chains created will be able to serve as macromonomers.

As ν is independent of the length or number of branch points on the main chain, the above derivation is rigorously valid as long as there is in the system enough unsaturated chains to be used as macromonomers. The limitation of the Monte Carlo based method occurs when the number of vinyl-terminated chains becomes smaller than the total number of branch points in the system. The average number of branch point which the catalyst will create before terminating the chain is simply the ratio of P_b, the probability of occurrence of a branch point, over $(1 - P_b)$, the probability of completing a chain. The condition of applicability then reads:

$$\frac{P_b}{1 - P_b} = \frac{\mathrm{pp}(1 - \mathrm{lp})}{1 - \mathrm{pp}} \leq \nu \tag{37}$$

This condition on lp becomes more restrictive than eq 35 and therefore becomes the only necessary condition:

$$\mathrm{lp} > 2 - \frac{1}{\mathrm{pp}} + (1 - \nu)\frac{1 - \mathrm{pp}}{\mathrm{pp}} \tag{38}$$

This means that if eq 38 is obeyed, Monte Carlo simulations obtained from pp, lp, and ν will represent a possible branched metallocene system.

Although these three parameters appear as independent in the simulation, they cannot be controlled independently in the reactor. For instance in the case one wants to study the influence of the rate of vinyl termination, the parameter lp cannot be kept constant since the probability of incorporating a macromonomer depends on the amount of available vinyl-terminated chains. The dependence of lp on ν can be obtained in the following way.

First the monomer selection probability is given using the notations of the kinetic reactions by

$$\mathrm{lp} = \frac{R_M}{R_M + R_{LCB}} = \frac{k_p M}{k_p M + k_{LCB} D^{=}} \tag{39}$$

where M is the concentration of monomers and $D^{=}$ is the total macromonomer concentration defined as

$$D^{=} = \sum_{x,n} D^{=}_{x,n} \tag{40}$$

We define the total concentration of dead chains, D^+, and the total concentration of terminated chains, D_0, as

$$D^+ = \sum_{x,n} D^+_{x,n} \text{ and } D_0 = D^{=} + D^+ \tag{41}$$

The vinyl termination probability ν is

$$\nu = \frac{D^{=}}{D_0} \tag{42}$$

If we define lp_0 as the value of lp when $\nu = 1$, which occurs when $D^{=} = D_0$, we have

$$\mathrm{lp}_0 = \frac{k_p M}{k_p M + k_{LCB} D_0} \tag{43}$$

Now if the rate of vinyl termination decreases, combining eqs 39 and 42, one gets

$$\frac{1}{\mathrm{lp}} = 1 + \nu \frac{k_{LCB} D_0}{k_p M} \tag{44}$$

We eliminate kinetic constants using eq 43, and obtain the following relation

$$\mathrm{lp} = \frac{\mathrm{lp}_0}{\mathrm{lp}_0 + \nu(1 - \mathrm{lp}_0)} \tag{45}$$

from which the evolution of LCB with rate of vinyl termination can be easily derived with help of eq 22.

Application of Statistical Model to Previously Studied Materials

Application of these results to actual branched metallocene PE samples brings more information about the topology of these materials than can be directly measured from existing analytical techniques. We consider four long chain branched metallocene polyethylenes (Table 2). These materials, labeled HDB1−4, have previously been thoroughly characterized in terms of molecular structure[7] and rheological properties.[7−10] For these materials we calculate β from eq 28 making use of the two measurable molecular quantities that we consider to be the most reliable, as explained below. The resulting segment fractions are reported in Figure 6. For this particular series of materials, since the segment molecular weights are comparable, ($M_{N,S} \sim 30\,000$) the comparison of segmental composition seen on the triangular diagram gives qualitative information about the rheological properties of these samples. It is consistent

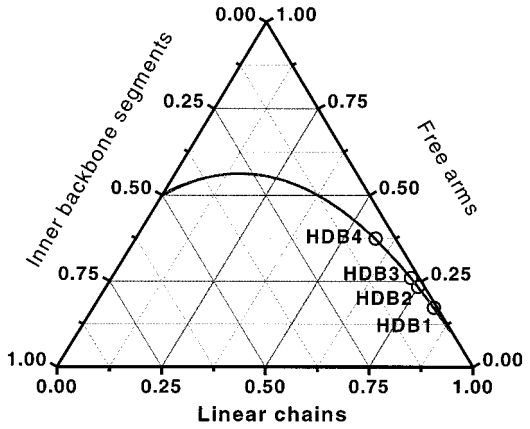

Figure 6. Ternary diagram with analytical solution and simulation results for HDB series.

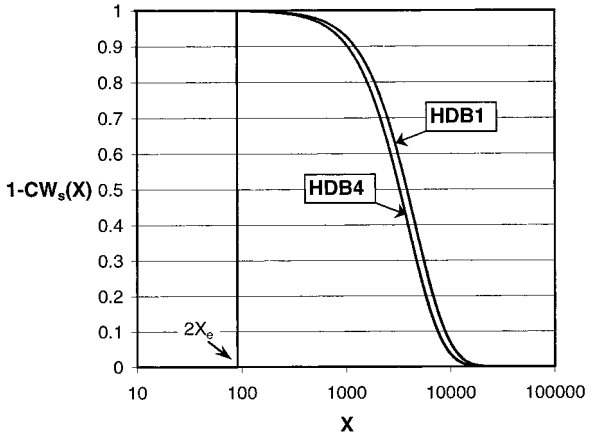

Figure 7. Weight fraction of segments with kinetic chain length greater than X as a function of X. Recall that $X = M/28$. The vertical line indicates the kinetic chain length at which the segments begin to affect the rheology. For all materials 99.9 wt % of the segments are longer than $2M_e$.

with the observed increase of viscosity from HDB1 to HDB4[7,8] and the fact that only HDB4, which has 5% inner segments, displays significant strain hardening. To determine the topological parameters β and $M_{N,S}$, two reliable experimental values must be chosen among the results of GPC, LALLS and NMR presented in Table 2. We assume that the light scattering measurement gives the best estimate of weight-average molecular weight as the universal calibration in combination with differential refractive index detectors is known to underestimate the molecular weight of long chain branched molecules. The reason for this is that the separation in size exclusion chromatography is according to hydrodynamic volume; larger molecules leave the column before smaller molecules. For linear polymers, hydrodynamic volume is uniquely related to molecular weight. This is not the case with polydisperse branched polymers such as LCB mPE, as fractions of constant hydrodynamic volume will consist of linear chains with a certain molecular weight and branched chains with higher molecular weights. Using GPC with a differential refractive index (DRI) detector results in an estimate of overall weight-average molecular weight for LCB mPE equal to the molecular weight of a linear system with the same weight-average hydrodynamic volume. In comparison a light scattering detector measures the weight-average molecular weight of each fraction leading to an accurate overall M_W.

Another difficulty arises when trying to measure the number-average molecular weight. Light scattering detectors are insensitive to low molecular weight molecules leading to a gross underestimation of the number-average molecular weight. The best estimate of number-average molecular weight comes from the differential refractive index (DRI) detector but this of course will contain the error due to the separation. The best estimate of the polydispersity index (M_W/M_N) is obtained by using the M_W from light scattering and the M_N from the DRI detector. This estimate agrees well to that predicted by eq 27 (Table 2) considering the level of error that we expect in M_N.

The next issue to address here is the discrepancy between the measurement of branch point density with ^{13}C NMR and the branches that are actually long enough to affect the rheology. NMR measures the density of methine carbons that are attached to three segments of more than five carbons in length. Only segments that are longer than twice the entanglement molecular weight, M_e, will affect the rheology.[11] For polyethylene, M_e is approximately 1250[12] or 90 carbons; thus, only the segments that are longer than 180 C will affect the rheology.

To estimate the fraction of long chain branches that do not affect the rheology we consider the segment weight molecular weight distribution given by eq 9 in its cumulative form:

$$CW_S(x) = 1 - \left[\frac{2x(\beta+1)(2\beta+1)}{M_W/28} + 1\right] \times \exp\left(\frac{-2x(\beta+1)(2\beta+1)}{M_W/28}\right) \quad (46)$$

Recall that the kinetic chain length, x, is equal to the number of monomers in the chain (M/28) and to half the number of carbons in the chain. Also, $CW_S(x)$ is the weight fraction of segments that have a kinetic chain length less than or equal to x. The kinetic chain length corresponding to $2M_e$ is 90 (i.e., 180 C) and therefore $CW_S(90)$ is the fraction of segments that do not affect the rheology. In Figure 7, we have plotted $[1 - CW_S(x)]$ for HDB1 and HDB4. For all materials studied here 99.9 wt % of the weight of the LCB measured by NMR can be expected to act as long branches in terms of the rheological properties.

Finally, we introduce the idea of a rheologically relevant branching parameter for these materials. In the past, ^{13}C NMR results (λ, LCB/10^3 C) have been used to rank materials in terms of their level of long chain branching[7]. Equation 28 shows clearly that a single value of λ can result from an infinite set of β, M_W combinations each of which will have a different average segment molecular weight (and different seniority and priority distributions) and therefore different rheological properties. We propose that the weight-average weight of branches per molecule, $\beta M_{W,S}$, is a more useful parameter for correlating with rheological properties. This parameter incorporates the effect of segment molecular weight and would describe the rheological behavior exactly if there were no molecules with more than two branch points. As the weight fraction of molecules with three or more branch points increases with increasing β, we expect that for high β any correlation between a rheological property and $\beta M_{W,S}$ would begin to fail (note: $F_W(n)$ is plotted for HDB4 in

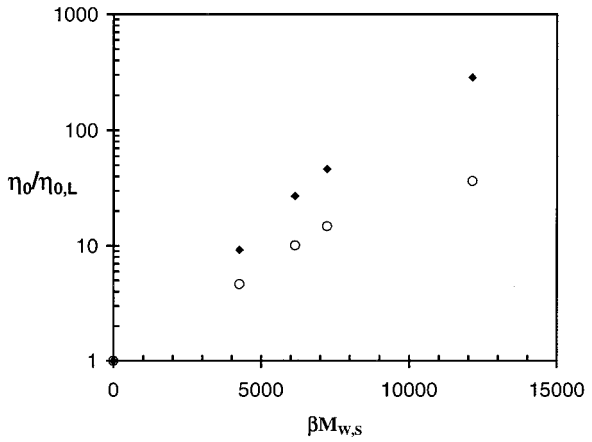

Figure 8. Correlation between zero shear viscosity enhancement (150 °C) and average mass of arms per molecule. Zero shear viscosity of linear polyethylene was calculated using the relation presented in ref 7. Filled symbols indicate viscosity enhancement with respect to a linear polyethylene of $M_W = M_{W,S}$ and open symbols indicate viscosity enhancement with respect to a linear polyethylene of the same M_W.

Figure 12). We demonstrate this in Figure 8 where the zero shear viscosity enhancement is plotted against $\beta M_{W,S}$. This relationship is linear on the semilog plot for low β and then curves over in the case of HDB4. Nevertheless, this correlation is much more useful than correlations involving only λ, and we demonstrate in the next section how we might use it to estimate the zero shear viscosity of blended systems.

Blended Systems

Blends of polymers are often used in applications where desired properties cannot be obtained with a single resin. Metallocene polymers are ideal candidates for blending due to the ease of producing well-defined molecular structures. In this section we present guidelines for making use of our branching architecture analysis for blends of several single-catalyst mPEs and for blends of single-catalyst mPEs with other linear polyethylenes.

We first consider a blend of N resins with respective average number of branch points per molecule, β_i and weight-average molecular weight $M_{W,i}$. Recall that in the single-catalyst mPE system there are two independent variables; we present our analysis in terms of β and M_W, but we could also choose to work with any other two molecular parameters. The number-average molecular weight of the blend is given by eq 47

$$\hat{M}_N = \left[\sum_{i=1}^{N} \frac{\omega_i}{M_{N,i}}\right]^{-1} \tag{47}$$

where the hat refers to a blend and ω_i is the weight fraction of component i in the blend. In the case of blends of multiple mPE resins, eq 48 also applies:

$$\hat{M}_N = \left[\sum_{i=1}^{N} \frac{2\omega_i(\beta_i + 1)}{M_{W,i}}\right]^{-1} \tag{48}$$

The weight-average molecular weight of the blend is given by

$$\hat{M}_W = \sum_{i=1}^{N} \omega_i M_{W,i} \tag{49}$$

To examine the various distributions in the blended system we must make use of the blend constituent composition in terms of number fraction, ν_i, which is related to the composition in weight fraction as follows:

$$\nu_i = \frac{\omega_i/M_{N,i}}{\sum_{i=1}^{N} \omega_i/M_{N,i}} \quad \text{for } i = 1-N \tag{50}$$

In the case of blends of multiple mPE resins eq 50 can be rewritten as

$$\nu_i = \frac{2(\beta_i + 1)\omega_i/M_{W,i}}{\sum_{i=1}^{N} 2(\beta_i + 1)\omega_i/M_{W,i}} \quad \text{for } i = 1-N \tag{51}$$

Then the branch point distributions are additive:

$$\hat{F}_N(n) = \sum_{i=1}^{N} \nu_i F_{N,i}(n) \tag{52}$$

as are the parameters β_A and β_B defined in eqs 31 and 33. The fractions of linear chains $\hat{\phi}_L$, of free arms $\hat{\phi}_A$, and of inner backbones $\hat{\phi}_B$ in the blend are then given by eq 53.

$$\hat{\phi}_\alpha = \frac{\sum_{i=1}^{N} \nu_i(2\beta_i + 1)\phi_{\alpha,i}}{\sum_{i=1}^{N} \nu_i(2\beta_i + 1)} = \sum_{i=1}^{N} k_i \phi_{\alpha,i} \quad \alpha = \text{L, A, B} \tag{53}$$

We see that the segment compositions as displayed in the ternary diagram are weighted by the number fraction of segments in the blend that come from component i, here called k_i. Making use of eq 50, we write k_i in terms of ω_i for blends of multiple mPE resins:

$$k_i = \frac{(2\beta_i + 1)2(\beta_i + 1)\omega_i/M_{W,i}}{\sum_{i=1}^{N} (2\beta_i + 1)2(\beta_i + 1)\omega_i/M_{W,i}} = \frac{\omega_i/M_{N,S,i}}{\sum_{i=1}^{N} \omega_i/M_{N,S,i}} \tag{54}$$

In eq 54, $M_{N,S,i}$ is the number-average molecular weight of the segments in component i. The inverse relationship can be used to obtain the weight fractions from a point on the ternary diagram:

$$\omega_i = \frac{k_i M_{N,S,i}}{\sum_{i=1}^{N} k_i M_{N,S,i}} \tag{55}$$

The simplest way to represent the composition of a binary blend is to draw a tie line between the two points on the ternary diagram that represent the two blend components. For example, consider the blending of two

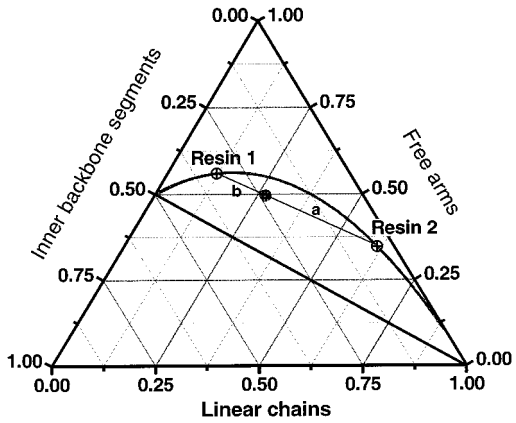

Figure 9. Composition of a blend of two metallocene resins.

long chain branched mPEs (resin 1 and resin 2) shown on the ternary diagram in Figure 9. The blend composition (in weight fraction) will fall on the tie line with its exact location determined by the lever rule:

$$\frac{a}{a+b} = k_2 = \frac{(2\beta_2+1)2(\beta_2+1)\omega_2/M_{W,2}}{\sum_{i=1}^{2}(2\beta_i+1)2(\beta_i+1)\omega_i/M_{W,i}}$$

$$\frac{b}{a+b} = k_1 = \frac{(2\beta_1+1)2(\beta_1+1)\omega_1/M_{W,1}}{\sum_{i=1}^{2}(2\beta_i+1)2(\beta_i+1)\omega_i/M_{W,i}} \quad (56)$$

In eq 56, a and b are the distances shown in Figure 9. The line connecting the 100% linear point with the 50% free arms and 50% inner backbone segments point is the limit below which compositions are physically impossible (there must be at least one more free arm than inner backbones in the system).

The rheological properties of the blended system will depend on the segment composition ($\hat{\phi}_\alpha$) and on the molecular weight distribution of the segment types. Therefore, it will also be necessary to consider these distributions. Let us consider a general blended system in which components 1 through m are single-catalyst long chain branched mPEs and components $m+1$ through N are linear polyethylenes (of any kind). The weight molecular weight distribution of the linear segments in such a system is given by eq 57

$$\hat{w}_L(x) = \frac{\sum_{i=1}^{m}\omega_i\phi_{L,i}x(1-p_i)^2(p_i)^{x-1}}{\sum_{k=1}^{m}\omega_k\phi_{L,k}} + \sum_{j=m+1}^{N}\omega_j w_j(x) \quad (57)$$

where

$$p_i = 1 - \frac{2(\beta_i+1)(2\beta_i+1)^2}{M_{W,i}/28} \quad (58)$$

and the subscript L refers to linear segments. The weight-average molecular weight of the linear segments is

$$\hat{M}_{W,L} = \frac{\sum_{i=1}^{m}\omega_i\phi_{L,i}\dfrac{M_{W,i}}{(\beta_i+1)(2\beta_i+1)}}{\sum_{k=1}^{m}\omega_k\phi_{L,k}} + \sum_{j=m+1}^{N}\omega_j M_{W,j} \quad (59)$$

The weight distributions of the free arms and inner segments is given by eq 60

$$\hat{w}_A(x) = \frac{\sum_{i=1}^{m}\omega_i\phi_{A,i}x(1-p_i)^2(p_i)^{x-1}}{\sum_{j=1}^{m}\omega_j\phi_{A,j}}$$

$$\hat{w}_B(x) = \frac{\sum_{i=1}^{m}\omega_i\phi_{B,i}x(1-p_i)^2(p_i)^{x-1}}{\sum_{j=1}^{m}\omega_j\phi_{B,j}} \quad (60)$$

where p_i is given by eq 58. The weight-average molecular weights of these segments are then

$$\hat{M}_{W,A} = \frac{\sum_{i=1}^{m}\omega_i\phi_{A,i}\dfrac{M_{W,i}}{(\beta_i+1)(2\beta_i+1)}}{\sum_{j=1}^{m}\omega_j\phi_{A,j}}$$

$$\hat{M}_{W,B} = \frac{\sum_{i=1}^{m}\omega_i\phi_{B,i}\dfrac{M_{W,i}}{(\beta_i+1)(2\beta_i+1)}}{\sum_{j=1}^{m}\omega_j\phi_{B,j}} \quad (61)$$

Consider the example shown in Figure 10, where two possible ways of making a blend with the same segment composition are shown. In the first case, the blend is made by combining two LCB mPEs with different β, and in the second case, the blend is made by combining one LCB mPE with a linear mPE. Even though these two blends will fall on the same point on the ternary diagram, they could have very different segment molecular weight distributions and segment seniority distributions and therefore different rheological properties. To obtain an approximate estimate of the zero shear viscosity of a blend, one might use the results in Figure 8 to estimate the zero shear viscosity of the pure components and then use a blending rule to calculate the zero shear viscosity of the blend. A similar approach could be used with other rheological properties as we will address in future work.

Of central concern is how to plan the composition of a blend to give the desired properties. Here we consider only the rheological properties and present general

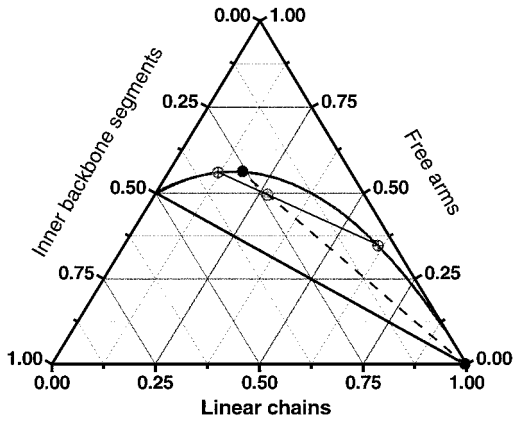

Figure 10. Two alternate blends with the same segment composition.

guidelines. Future work is planned to present a more concrete analysis. Aside from melt fracture behavior, the two most important rheological properties are the viscosity under processing conditions and the strain hardening nature of the extensional viscosity. Simply stated, free arms increase the viscosity of the system (relative to a linear system of the same molecular weight) without causing significant strain hardening. Only the inner segments contribute to strain hardening, and the higher the priority of the inner segment, the more it contributes to strain hardening.[4] Linear chains dilute the effects of both the free arms and the inner segments. Generally, an increased viscosity has a negative impact on the processing operation, and increased strain hardening has a positive impact on the processing operation.

In a single-catalyst long chain branched mPE the only way to increase the amount of inner segments is to move along the curve in the ternary diagram, which necessarily results in an increase in the amount of free arms, and therefore an enormous increase in the viscosity. To decrease the viscosity while maintaining some of the strain hardening one can move from the curve by blending. To optimize the processing behavior the segment composition of the blend should be as close as possible to the limiting line ($\phi_B/\phi_A = 1$) and as far as possible from the purely linear system ($\phi_L = 1$). The limiting factor will be the handling of the high β component prior to blending.

Now we must also mention that while blending provides one way of increasing the utility of metallocene polyethylenes it will not provide all of the answers. The next step of course is to consider multiple-metallocene-catalyst systems, which will provide many more possible structures and also perhaps improved processability.

Conclusions

A practical framework for the analysis of the branching architecture of metallocene polyethylenes is presented. An analytical solution of the statistics is presented in a form relevant to rheology−chain structure relations. This solution was verified using rigorous Monte Carlo simulations. For long chain branched polyethylene synthesized with single-site catalysts, we find that the most useful parameter for describing the branching structure is the average number of branch points per molecule, which can be determined from the combination of light scattering and ^{13}C NMR measurements.

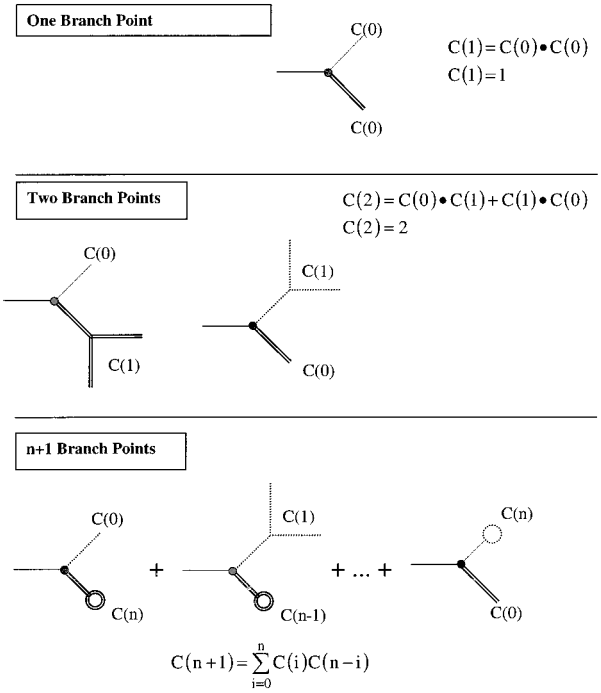

Figure 11. Counting configurations for molecules

Acknowledgment. Funding was provided by The Dow Chemical Co. and the Natural Sciences and Engineering Research Council of Canada.

Appendix A: The Catalan Numbers

To develop relations for the various distributions in the system, we need to consider the number of ways a molecule of n branch points can be produced in the polymerization process. For example a linear chain can be formed in only one way; by not incorporating any macromonomers; thus, $C(0) = 1$. Likewise, a chain with a single branch point can only be formed by incorporating a single linear macromonomer; $C(1) = 1$. However, a chain with two branch points can be formed either by incorporating two linear macromonomers or by incorporating a single macromonomer that has one branch point; $C(2) = 2$.

For more than two branch points, the preceding approach to counting the possible ways of constructing a molecule becomes inefficient, and a more useful approach is presented in Figure 11. In this approach, we choose a segment to focus on (indicated in the figure by a solid line) and make up the rest of the molecule by adding one linear chain and one chain with $(n - 1)$ branch points. This gives a structure that can be constructed in $C(0)C(n - 1)$ different ways. We then make the next structure by returning to our original segment and adding one chain with a single branch point and one chain with $(n - 2)$ branch points. This structure can be constructed in $C(1)C(n - 2)$ different ways. We continue making different structures until we end up with a chain with $(n - 1)$ branch points in the original position of the linear chain and a linear chain in the original position of the chain with $(n - 1)$ branch points. Then the number of ways that the molecule of n branch points can be constructed is the sum over all of

the structures:

$$C(n) = \sum_{i=0}^{n-1} C(i)C(n-1-i) \tag{A1}$$

The solution to the previous recursive equation, the Catalan numbers, was found by Catalan in 1838

$$C(n) = \frac{(2n)!}{n!(n+1)!} \tag{A2}$$

as the coefficients in the development of the generating function[13]

$$\sum_{n=0}^{\infty} C(n)z^n = \frac{1-\sqrt{1-4z}}{2z} = G(z) \tag{A3}$$

This result originally was applied by Flory[6] to solve an relation similar to eq A1 in the case of random branching of linear chains describing the sol−gel transition for molecules with functionality 3. Although the polymerization process that we are considering is different, the number of ways to create a molecule with n branch points is the same. The above equations can be used to derive eq 18 in the text. According to the definition of the average number of branch points per chain

$$\beta = \sum_{n=1}^{\infty} nC(n){P_b}^n(1-P_b)^{n+1} = (1-P_b)\sum_{n=1}^{\infty} nC(n)[P_b(1-P_b)]^n \tag{A4}$$

As

$$\frac{dG}{dz} = G'(z) = \sum_{n=1}^{\infty} nC(n)z^{n-1} = \frac{1-2z-\sqrt{1-4z}}{2z^2\sqrt{1-4z}} \tag{A5}$$

we can write

$$\beta = P_b(1-P_b)^2 G'(P_b(1-P_b)) \tag{A6}$$

In the present case, $P_b < {}^1/_2$ which implies that $P_b(1-P_b) < {}^1/_4$.

Therefore

$$\sqrt{1-4P_b(1-P_b)} = 1-2P_b \tag{A7}$$

Then

$$\beta = P_b(1-P_b)^2\frac{1-2P_b(1-P_b)-(1-2P_b)}{2(P_b(1-P_b))^2(1-2P_b)} = \frac{P_b}{1-2P_b} \tag{A8}$$

Appendix B: Molecular Weight Distribution for Molecules of *n* Branch Points

We now wish to find the MWD for molecules with n branch points. The probability $P(x,n)$ for having $2n+1$ segments of kinetic length x_i ($1 \le i \le 2n+1$) each with distribution n_S and a total degree of polymerization equal to x is

$$P(\{x_i\},n) = \prod_{i=1}^{2n+1} n_S(x_i) \quad \text{with } x = \sum_{i=1}^{2n+1} x_i \tag{B1}$$

This can be rewritten by using:

$$x_{2n+1} = x - \sum_{i=1}^{2n} x_i \tag{B2}$$

to give:

$$P(\{x_i\},n) = n_S(x - \sum_{i=1}^{2n} x_i)\prod_{i=1}^{2n} n_S(x_i)$$

$$P(\{x_i\},n) = (1-p)^{2n+1}p^{(x-\sum_{i=1}^{2n}x_i-1)}\prod_{i=1}^{2n} p^{x_i-1} \tag{B3}$$

In eq B3, the probability $p = \text{pp} \times \text{lp}$. The distribution is then obtained by summing on all possible values of x_i between 1 and x:

$$P(x,n) = (1-p)^{2n+1}p^{x-\sum_{i=1}^{2n}x_i-1}\int_1^x \prod_{i=1}^{2n} dx_i\, p^{x_i-1} = (1-p)^{2n+1}p^{x-(2n+1)}\int_1^x \prod_{i=1}^{2n} dx_i \tag{B4}$$

Actually, the integral must be written as

$$\int_1^x \prod_{i=1}^{2n} dx_i = \prod_{i=1}^{2n}\int_1^{\xi_i} dx_i \tag{B5}$$

where the boundary ξ_i is

$$\xi_i = x - \sum_{j=1}^{i-1} x_i - (2n+1-i) \tag{B6}$$

Since each segment must contain at least one monomer, the length of x_1 must therefore be chosen between 1 and $\xi_1 = x - 2n$, since there remain $2n$ more segments. Then x_2 varies between 1 and $\xi_2 = x - x_1 - (2n-1)$, x_3 until $\xi_3 = x - (x_1 + x_2) - (2n-2)$ and x_{2n} until $\xi_{2n} = x - (x_1 + \ldots + x_{2n-1}) - 1$. The integral part of eq B4 is then exactly given by eq B7.

$$\int_1^{x-2n} dx_1 \int_1^{x-x_1-(2n-1)} dx_2 \ldots \int_1^{x-(x_1+\ldots+x_{2n-1})-1} dx_{2n} = \frac{(x-(2n+1))^{2n}}{(2n)!} \tag{B7}$$

Finally, the number MWD of molecules with n branch points before normalization is

$$P(x,n) = \frac{1}{(2n)!}(1-p)^{2n+1}p^{x-(2n+1)}(x-(2n+1))^{2n} \tag{B8}$$

with $x \ge 2n+1$. As p is very close to 1, we can approximate the previous equation by

$$P(x,n) \approx \frac{1}{(2n)!}e^{-x(1-p)}(x-(2n+1))^{2n}\left(\frac{1-p}{p}\right)^{2n+1} \tag{B9}$$

and as x is usually significantly larger than $(2n + 1)$, we can further simplify to give

$$P(x,n) \approx \frac{1}{(2n)!}e^{-x(1-p)}x^{2n}\left(\frac{1-p}{p}\right)^{2n+1} \quad \text{(B10)}$$

After normalization by integration of $P(x,n)$ between $x = (2n + 1)$ and $x = +\infty$ for eqs B8 and B9 and between $x = 0$ and $x = +\infty$ for eq B10, the three relations are very similar. We can therefore use eq B10, which is easily normalized by making use of eq B11:

$$\int_0^{+\infty} dx\, e^{-\alpha x}x^k = \frac{k!}{\alpha^{k+1}} \quad \text{(B11)}$$

Therefore, the normalized number, weight, and Z distributions of molecules with n branch points are given by eqs B12−B14.

$$P_N(x,n) = \frac{(1-p)^{2n+1}}{(2n)!}x^{2n}e^{-x(1-p)} \quad \text{(B12)}$$

$$P_W(x,n) = \frac{xP_N(x,n)}{\int_0^{\infty} xP_N(x,n)\,dx} = \frac{(1-p)^{2n+2}}{(2n+1)!}x^{2n+1}e^{-x(1-p)} \quad \text{(B13)}$$

$$P_Z(x,n) = \frac{xP_W(x,n)}{\int_0^{\infty} xP_W(x,n)\,dx} = \frac{(1-p)^{2n+3}}{(2n+2)!}x^{2n+2}e^{-x(1-p)} \quad \text{(B14)}$$

The average molecular weights are given by eqs B15−B17.

$$M_N(n) = \int_0^{\infty} xP_N(x,n)\,dx = \frac{2n+1}{1-p} = (2n+1)M_{N,S} \quad \text{(B15)}$$

$$M_W(n) = \int_0^{\infty} xP_W(x,n)\,dx = \frac{2n+2}{1-p} = (2n+2)M_{N,S} \quad \text{(B16)}$$

$$M_Z(n) = \int_0^{\infty} xP_Z(x,n)\,dx = \frac{2n+3}{1-p} = (2n+3)M_{N,S} \quad \text{(B17)}$$

The polydispersity indexes are $M_W(n)/M_N(n) = (2n + 2)/(2n + 1)$ and $M_Z(n)/M_N(n) = (2n + 3)/(2n + 1)$, which gives the classical results for the Flory distribution when $n = 0$.

Appendix C: Weight Distributions

We now present the most general description of the single-metallocene-catalyst system in terms of bivariate distributions. The bivariate number distribution is given by eq C1

$$f_N(x,n) = F_N(n)P_N(x,n) \quad \text{(C1)}$$

which can be written in terms of β by substituting in eqs 15 and B12 and making use of eq 14

$$f_N(x,n) = F_N(n)P_N(x,n) = \frac{x^{2n}e^{-x(1-pp\times lp)}}{n!(n+1)!}pp^n(1-lp)^n(1-pp)^{n+1} \quad \text{(C2)}$$

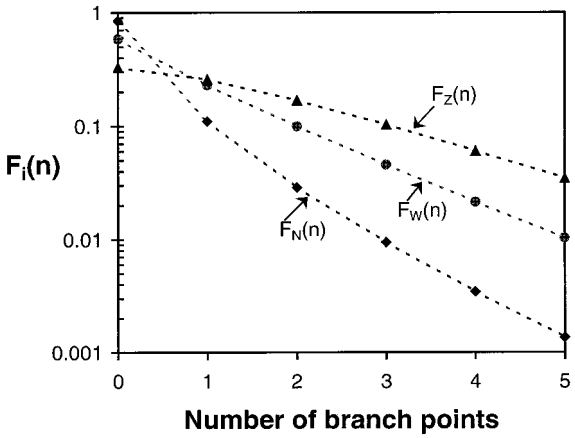

Figure 12. Number, weight, and Z fractions of molecules with n branch points in HDB4 ($\beta = 0.224$). The lines are drawn to aid the eye only and do not indicate the existence of these functions at noninteger values of n.

or using only $X_N = M_N/28$ and β as parameters:

$$f_N(x,n) = \frac{\beta^n(\beta+1)^{n+1}}{n!(n+1)!}\frac{x^{2n}}{X_N{}^{2n+1}}\exp\left[-(2\beta+1)\frac{x}{X_N}\right] \quad \text{(C2a)}$$

We recall that $1 - p = 1 - pp \times lp = 1/X_{N,S} = 2\beta + 1/X_N$.

To derive the weight and Z bivariate distribution, which are more relevant than the number distribution to describe, respectively, the rheological and scattering behaviors, the average molecular weights together with the weight and Z fractions of molecules with n branch points are also needed:

$$M_N = \sum_{n=0}^{\infty} F_N(n)M_N(n) = \frac{M_{N,S}}{1-2P_b} = (2\beta+1)M_{N,S} \quad \text{(C3)}$$

$$F_W(n) = \frac{F_N(n)M_N(n)}{M_N} = \frac{(2n+1)!}{n!(n+1)!}P_b{}^n(1-P_b)^{n+1}(1-2P_b) \quad \text{(C4)}$$

$$M_W = \sum_{n=0}^{\infty} F_W(n)M_W(n) = \frac{2(1-P_b)}{(1-2P_b)^2}M_{N,S} = 2(\beta+1)(2\beta+1)M_{N,S} \quad \text{(C5)}$$

$$F_Z(n) = \frac{F_W(n)M_W(n)}{M_W} = \frac{(2n+1)!}{(n!)^2}P_b{}^n(1-P_b)^n(1-2P_b)^3 \quad \text{(C6)}$$

$$M_Z = \sum_{n=0}^{\infty} F_Z(n)M_Z(n) = \frac{3}{(1-2P_b)^2}M_{N,S} = 3(2\beta+1)^2\,M_{N,S} \quad \text{(C7)}$$

$F_N(n)$, $F_W(n)$ and $F_Z(n)$ are plotted for $\beta = 0.224$ in Figure 12. The weight and Z bivariate distributions are

then given by

$$f_W(x,n) = F_W(n)P_W(x,n) = \frac{x^{2n+1}e^{-x(1-pp\times lp)}}{n!(n+1)!} \times pp^n(1-lp)^n(1-pp)^{n+1}(1-2pp+pp\times lp) \quad (C8)$$

or equivalently

$$f_W(x,n) = \frac{\beta^n(\beta+1)^{n+1}}{n!(n+1)!}\frac{x^{2n+1}}{X_N{}^{2n+2}}\exp\left[-(2\beta+1)\frac{x}{X_N}\right] = \frac{x}{X_N}f_N(x,n) \quad (C8a)$$

and

$$f_Z(x,n) = F_Z(n)P_Z(x,n) = \frac{x^{2n+2}e^{-x(1-pp\times lp)}}{n!(n+1)!} \times pp^n(1-lp)^n(1-pp)^n\frac{(1-2pp+pp\times lp)^3}{2} \quad (C9)$$

which leads to

$$f_Z(x,n) = \frac{1}{2}\frac{\beta^n(\beta+1)^n}{n!(n+1)!}\frac{x^{2n+2}}{X_N{}^{2n+3}}\exp\left[-(2\beta+1)\frac{x}{X_N}\right] = \frac{x}{X_W}f_W(x,n) \quad (C9a)$$

where $X_W = 2(\beta+1)X_N$.

By summing on n, one can get the overall number, weight, and Z distributions of the branched system:

$$N(x) = \sum_{n=0}^{\infty} f_N(x,n)W(x) = \sum_{n=0}^{\infty} f_W(x,n)\; Z(x) = \sum_{n=0}^{\infty} f_Z(x,n) \quad (C10)$$

This makes use of the identity

$$\sum_{n=0}^{\infty}\frac{(z/2)^{2n+1}}{n!(n+1)!} = I_1(z) \quad (C11)$$

where I_1 is the modified Bessel function of the first kind of order 1. Then the molecular weight distribution reads

$$W(x) = \frac{\sqrt{1+\beta^{-1}}}{X_N}\exp\left(-(2\beta+1)\frac{x}{X_N}\right)I_1\left(2\sqrt{\beta(\beta+1)}\frac{x}{X_N}\right) \quad (C12)$$

We note that x and X_N can be replaced with M and M_N respectively to get the normalized molecular weight distributions $W(M)$, and the number and Z distributions are related to $W(M)$ by the usual relations:

$$N(M) = \frac{M_N}{M}W(M) \quad (C13)$$

$$Z(M) = \frac{M}{M_W}W(M) \quad (C14)$$

These relations are important insofar as the experimental determination of molecular weight distributions of branched metallocene PE is extremely delicate: indeed, as shown by Zimm and Stockmayer,[14] molecules with different molecular weights can be eluted at the same time, provided that they have different numbers of branch points. Unfortunately, correcting the GPC curve for branch systems requires knowledge of the topology. This justifies why the determination of branching density from average molecular weights, as suggested by eqs 27 and 28, is not practically achievable.

Appendix D: Apparent Percolation Threshold

As β approaches ∞, i.e., when $P_b = {}^1/_2$ the system approaches an apparent percolation. The number fraction of molecules with n branch points is given by eq D1 for $n > 0$.

$$F_N(n) = \frac{2n(2n-1)}{n(n+1)}P_b(1-P_b)F_N(n-1) = \frac{2n-1}{2n+2}F_N(n-1) \quad (D1)$$

For $n = 0$

$$F_N(0) = 1 - P_b = {}^1/_2 \quad (D2)$$

By using the Stirling formula $n! \approx n^{(n+1/2)}e^{-n}\sqrt{2\pi}$, one can show that for large n, $F_N(n) \propto n^{-3/2}$ and $F_W(n) \propto n^{-1/2}$. Thus, both functions are decreasing with increasing n. Even at the limit $\beta \to \infty$, half the chains are linear, and there are more three-arm stars than any other branched structures. The ranking is the same in terms of weight fractions, although the differences between the weight fractions of the various structures are less. Therefore, this is not properly speaking a percolation. Nevertheless, the average molecular size diverges and the fraction of linear chains becomes negligible compared to the fraction of free arms and inner backbones. As explained in the text, the limit $\beta \to \infty$ can only be considered when all chains formed are vinyl terminated.

Nomenclature of Principal Symbols

β = average number of branch points per chain
λ = branching density [LCB/10^3 C]
ϕ_L, ϕ_A, ϕ_B = fractions of linear segments, free arms, and inner backbones
$\hat{\phi}_L$, $\hat{\phi}_A$, $\hat{\phi}_B$ = fractions of linear, free arms, and inner backbones in a blend
ν_i, ω_i = number and weight composition of a blend for component i
$C(n)$ = Catalan numbers
$f_N(x,n)$, $f_W(x,n)$, $f_Z(x,n)$ = number, weight, and Z bivariate distributions
$F_N(n)$, $F_W(n)$, $F_Z(n)$ = number, weight, and Z fraction of molecules with n branch points
lp = monomer/macromonomer selection probability
M = molecular weight
M_e = average weight between entanglements (1250 for PE)
M_0 = monomer molecular weight (28 for PE)
M_N, M_W, M_Z = number-, weight-, and Z-average molecular weights of resin
$\hat{M}_N$, $\hat{M}_W$ = number and weight molecular weights of a blend
$M_{N,S}$, $M_{W,S}$ = number- and weight-average molecular weights of segments
$M_N(n)$, $M_W(n)$, $M_Z(n)$ = average molecular weights of molecules with n branch points
$N(M)$, $W(M)$, $Z(M)$ = number, weight, and Z molecular weight distributions
n = number of branch points
$n_S(x)$ = segment number distribution of kinetic length
$CN_S(x)$ = cumulative segment number distribution of kinetic length
P_b = Flory branching probability

PDI = polydispersity index
$P_N(x,n)$, $P_W(x,n)$, $P_Z(x,n)$ = number, weight, and Z MWD of molecules with n branch points
pp = propagation probability
R_p, R_t, R_{LCB}, R_{CTA}, R_β = kinetic rates
v = vinyl termination probability
$w_S(x)$ = segment weight distribution of kinetic length
$CW_S(x)$ = cumulative segment weight distribution of kinetic length
x = kinetic length (M/M_0)
X_N, X_W = number- and weight-average kinetic length of resin

References and Notes

(1) Soares, J. P. B.; Hamielec, A. E. *Macromol. Theory Simul.* **1996**, *5*, 547.
(2) Beigzadeh, D.; Soares, J. B. P.; Duever, T. A.; Hamielec, A. E. *Polym. React. Eng. J.* **1999**, *7*, 195.
(3) Yannoulakis, H.; Yiagopoulos, A.; Pladis, P.; Kiparissides, C. *Macromolecules* **2000**, *33*, 2757.
(4) Read, D. J.; McLeish, T. C. B. *Macromolecules* **2001**, *34*, 1928.
(5) Flory, P. J. *Chem. Rev.* **1946**, *39*, 137.
(6) Flory, P. J. *J. Am. Chem. Soc.* **1941**, *63*, 3091.
(7) Wood-Adams, P. M.; Dealy, J. M.; deGroot, A. W.; Redwine O. D. *Macromolecules* **2000**, *33*, 7489.
(8) Wood-Adams, P. M. *J. Rheol.* **2000**, *45*, 203.
(9) Wood-Adams, P. M.; Dealy, J. M.; Costeux, S. *Polym. Mater.: Sci. Eng.* **2001**, *84*, 442.
(10) Wood-Adams, P. M.; S. Costeux, *Macromolecules* **2001**, *34*, 6281.
(11) Gell, C. B.; Graessley, W. W.; Efstratiadis, V.; Pitsikalis, M.; Hadjichristidis, N. *J. Polym. Sci., Part B: Polym. Phys.* **1997**, *35*, 1943.
(12) Raju, V. R.; Rachapudy, H.; Graessley, W. W. *J. Polym. Sci., Phys. Ed.* **1979**, *17*, 1223.
(13) Wilf, H. S. *Generatingfunctionology*; Academic Press: Boston, MA, 1990.
(14) Zimm, B. H.; Stockmayer, W. H. *J. Chem. Phys.* **1949**, *17*, 1301.

MA011432C